# Characterization of Phases Formed in the Iron Carbide Process by X-Ray Diffraction, Mossbauer, X-Ray Photoelectron Spectroscopy, and Raman Spectroscopy Analyses

EUNGYEUL PARK, JIANQIANG ZHANG, STUART THOMSON, OLEG OSTROVSKI, and RUSSELL HOWE

Iron carbide was prepared by iron ore reduction and iron cementation using Ar-$H_2$-$CH_4$ gas mixture with and without sulfur. Phases formed in the reduction/cementation process were examined by X-ray diffraction (XRD), Mossbauer, and Raman spectroscopy. The sample surface was also analyzed by X-ray photoelectron spectroscopy (XPS). XRD and Mossbauer analyses showed that iron oxide was first reduced to metallic iron, and then, metallic iron was carburized to cementite. Addition of a small amount of $H_2S$ to the reaction gas retarded the cementite formation but made the cementite more stable. XPS analysis showed that the surface of samples converted to iron carbide using sulfur-containing gas consisted of mainly $Fe_3C$ and a small amount of graphitic carbon. Raman spectra of a sample produced in the iron carbide process showed the *G* and *D* bands, which are characteristic for carbon-carbon bonds. The intensity ratio of *G*/*D* bands depended on the sulfur content in the reducing/carburizing gas.

## I. INTRODUCTION

THE iron carbide process has been developed as an alternative ironmaking process, in which iron ore fines are reduced by hydrogen-methane gas mixture in a fluidized bed reactor at relatively low temperature.[1–8] The iron carbide process has some advantages over the conventional blast furnace (BF)-ironmaking, which includes a coke oven, sinter plant, and BF itself. Its main by-product is water vapor. Fine iron ore can be processed directly, thereby eliminating the agglomeration stage. The product, iron carbide, is nonpyrophoric, which makes it safe and easy to store and transport. It is an attractive feed material for electric arc furnace (EAF) steelmaking, as combustion of carbon decreases the electric energy consumption, makes EAF slag to foam, and decreases the content of dissolved nitrogen. However, the iron carbide process needs further development. Nucor Corporation recently announced the closure of the only commercial iron carbide plant in Trinidad because of numerous engineering and quality problems. This emphasizes the necessity of further research in fundamentals of iron carbide formation, which was undertaken in this project.

Iron carbide production by reaction of iron ore with $CH_4$-$H_2$-Ar gas proceeds in two stages. Stage one involves the reduction of hematite to metallic iron. The second stage is a cementation of metallic iron by methane. Cementite formation can be presented by the reaction

$$3Fe_2O_3(s) + 5H_2(g) + 2CH_4(g) = 2Fe_3C(s) + 9H_2O(g) \quad [1]$$

In the iron carbide process, hematite is first quickly reduced by hydrogen to magnetite, and then, magnetite is reduced further to metallic iron when the temperature is below 568 °C. Methane is adsorbed on the surface of freshly formed metallic iron. Iron catalyzes the process of methane cracking with formation of carbon that is dissolved in iron. In the highly carburizing gas atmosphere, iron is supersaturated with carbon, which results in cementiite formation. However, cementite is metastable and decomposes to iron and carbon (soot). Sulphur, as a surface-active element, strongly affects the iron carbide process. A small amount of sulfur in the reaction gas retards iron ore reduction and iron cementation processes, and stabilizes iron carbide. However, mechanisms of cementite formation and the effects of sulphur on iron carbide process have not been well established. The characterization of phases formed in the iron carbide process is of importance for an understanding of the mechanisms of this process.

This article discusses characterization of phases formed in the iron carbide process by X-ray diffraction (XRD), Mossbauer, X-ray photoelectron spectroscopy (XPS), and Raman spectroscopy.

## II. EXPERIMENTAL

### A. *Sample Preparation*

Samples were prepared by reduction of iron ore using a $CH_4$-$H_2$-Ar gas mixture in a laboratory, isothermal, fixed-bed reactor in a vertical-tube electric furnace. A schematic of the experimental reactor used in this research is presented in Figure 1. The $CH_4$-$H_2$-Ar gas mixture was prepared from purified argon, methane, and hydrogen using Brooks gas flow meters with electronic controllers (Model 5850E). The

EUNGYEUL PARK, Postgraduate Student, and OLEG OSTROVSKI, Professor, are with the School of Materials Science and Engineering, University of New South Wales, Sydney 2052, Australia. JIANQIANG ZHANG, Postdoctoral Research Fellow, is with the Max-Planck-Institute für Eisenforschung GmbH, D-40074 Dusseldorf, Germany. STUART THOMSON, Postdoctoral Research Fellow, is with the Max-Planck-Institute für Kohlenforschung, D-45470 Mulheim, Germany. RUSSELL HOWE, Professor, is with the Chemistry Department, University of Aberdeen, Aberdeen AB24 3UE, Scotland.

Manuscript submitted November 20, 2000.

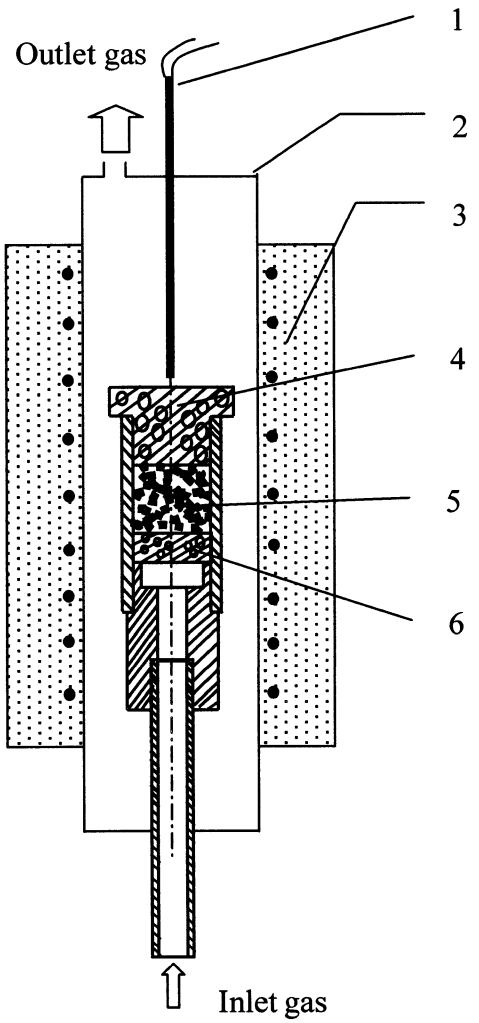


Fig. 1—Schematic of experimental setup and reactor: 1—thermocouple, 2—working tube, 3—furnace, 4—porous lid, 5—sample, and 6—bottom porous plug.

**Table I. Chemical Composition of the Iron Ore (Weight Percent)**

| Total Fe | $SiO_2$ | $Al_2O_3$ | $TiO_2$ | P | Mn | S |
|---|---|---|---|---|---|---|
| 62.7 | 4.81 | 2.61 | 0.08 | 0.087 | 0.04 | 0.026 |

reducing/carburizing gas was introduced into the reactor through a porous plug at the bottom of the reactor. The total gas flow rate was maintained at $10^{-3}$ $m^3$/min. In some experiments, sulfur was added into the gas mixture in the form of $H_2S$ supplied in the mixture with argon.

The iron ore composition is given in Table I. The ore was sized from 0.35 to 0.5 mm. The samples of iron ore subjected to reduction/cementation were 2 g.

The experimental procedure was as follows. A sample was heated in an argon atmosphere to the required temperature. Then, the reaction gas was introduced. The exit gas was analyzed online by a Fissons mass-spectrometer. After reduction, the sample was quenched by pulling down to a cold zone.

A Nucor iron carbide sample was also examined. 90 wt pct of the total iron in this sample was present in the form of iron carbide, 8 wt pct of the total iron was in the form of iron oxide, and 2 wt pct was metallic iron. The total carbon content was 6.2 wt pct, and the sample also contained 2 wt pct gangue materials.

### B. *X-ray Diffraction*

Samples were subjected to XRD analysis using a Siemens D5000, powder diffractometer with nickel-filtered Cu $K_\alpha$-radiation. The voltage and current were set at 30 kV and 30 mA. The scanning speed and step size were 0.6 deg/min and 0.01 deg, respectively.

### C. *Mossbauer Spectroscopy*

The Mossbauer spectra were recorded at room temperature on a constant acceleration and conventional standard transmission spectrometer with a 15 mCi $^{57}$CoRh source. The drive velocity scale was calibrated with a 12-$\mu$m-thick, pure $\alpha$-Fe foil (magnetic hyperfine field $B_{hf}$ = 33 T). The transmission of $\gamma$-rays through the absorber was detected using a Krypton-filled proportional detector. The resulting Mossbauer spectrum was accumulated by a multichannel analyzer, with 512 channels, and stored in the computer system for subsequent analysis. All isomer shifts were quoted relative to the center of the $\alpha$-Fe calibration spectrum. The experimental $^{57}$Fe Mossbauer spectra were fitted by a least-squares fitting procedure using the $^{57}$Fe Mossbauer fitting program.

### D. *X-Ray Photoelectron Spectroscopy*

Sample particles were compacted into a thin disk about 1-mm thick under a pressure of 1000 N/cm$^2$ and examined by a KRATOS XSAM800 instrument. The Mg $K_\alpha$(1253.6 eV) line was used for the X-ray source. The surfaces of the prepared samples were ion-beam etched for 15 minutes (Ar pressure: $10^{-7}$ torr). The pressure of the analysis chamber during measurement was $5 \times 10^{-9}$ torr.

### E. *Raman Spectroscopy*

The samples were analyzed by a Renishaw Raman microprobe in air at room temperature. The laser beam was perpendicular to the analyzed surface. All spectra were taken using the 514 nm line of an Ar ion laser.

## III. RESULTS AND DISCUSSION

### A. *XRD Analysis*

X-ray diffraction patterns of samples reduced/carburized at 750 °C and 835 °C are shown in Figures 2 and 3, respectively. The reducing/carburizing gas consisted of 35 vol pct $CH_4$, 55 vol pct $H_2$, and 10 vol pct Ar. Results obtained at 750 °C are summarized in Table II.

Hematite was first reduced to magnetite and, then, to wustite and metallic iron. It took less than 15 minutes at 750 °C and 10 minutes at 835 °C to reduce iron oxide to metallic iron. Further increase in reaction time led to cementite formation. At 750 °C, iron was almost completely converted to iron carbide in 30 minutes. Cementite is an unstable phase and decomposes to metallic iron and solid carbon

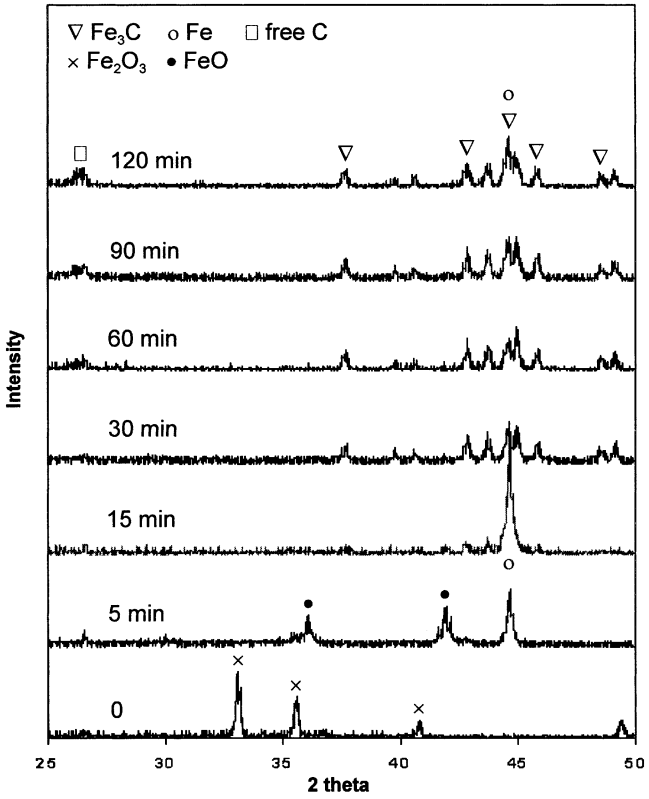


Fig. 2—XRD patterns of samples reduced at 750 °C with $CH_4$-$H_2$-Ar gas (35 vol pct $CH_4$, 55 vol pct $H_2$, and 10 vol pct Ar) at different reduction times.

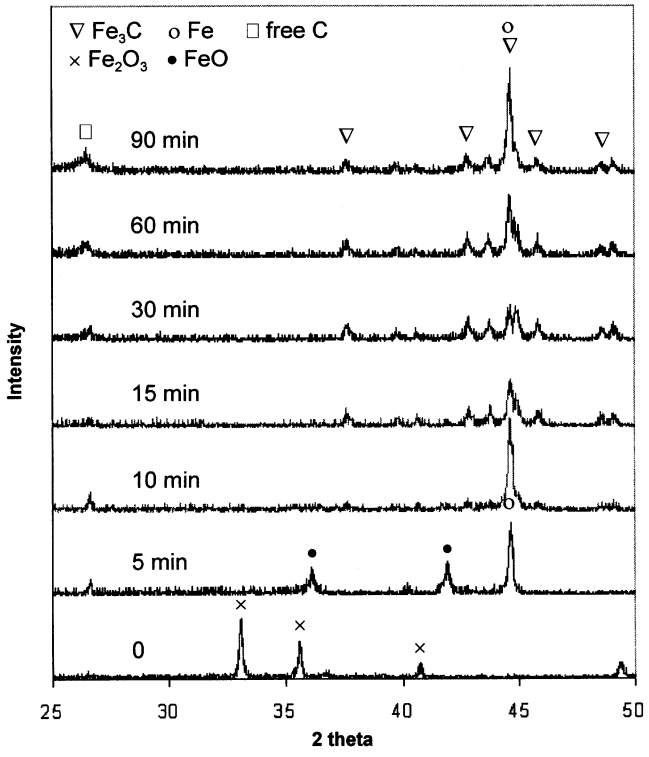


Fig. 3—XRD patterns of samples reduced at 835 °C with $CH_4$-$H_2$-Ar gas (35 vol pct $CH_4$, 55 vol pct $H_2$, and 10 vol pct Ar) at different reduction times.

even in the strongly carburizing atmosphere. The mechanism of cementite decomposition is similar to the mechanism of iron dusting suggested by Grabke.[9] At 750 °C, decomposition started after 2 hours of reaction. While at 835 °C, decomposition of cementite started after 15 minutes of reaction, and most of the cementite decomposed into metallic iron and free carbon after about 1.5 hours.

**Table II. XRD Analysis of Iron Ore Reduced and Carburized at 750 °C (Weight Percent)**

| Reaction Time (Min) | $Fe_3O_4$ | FeO | Fe | $Fe_3C$ |
|---|---|---|---|---|
| 5 | 0 | 56.8 | 43.2 | 0 |
| 15 | 0 | 8.2 | 74.7 | 17.1 |
| 30 | 0 | 0 | 0 | 100 |
| 60 | 0 | 0 | 0 | 100 |
| 90 | 0 | 0 | 0 | 100 |
| 120 | 0 | 0 | 9.9 | 90.1 |

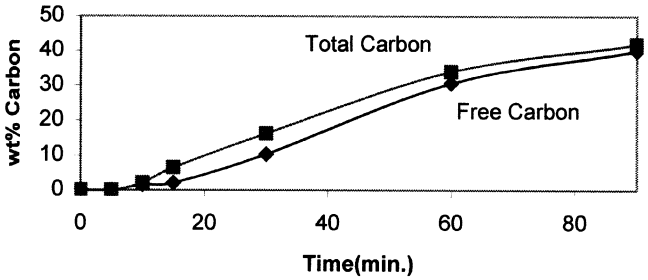


Fig. 4—Total and free carbon content in samples reduced at 835 °C as a function of the reduction time.

The free solid carbon was formed as a result of methane cracking and cementite decomposition. Its content was obtained as the difference between the total carbon content in a sample measured by a LECO* CS-244 carbon-sulfur detector and the carbon content in cementite. The free carbon content in a sample reduced at 835 °C to different extents is plotted as a function of reaction time in Figure 4. Its content increased with time.

*LECO is a trademark of LECO Corporation, St. Joseph, MI.

The XRD patterns of samples reduced/carburized at 925 °C in the gas atmosphere containing sulfur are shown in Figure 5. The reaction time was 1 hour for all samples. When the gas atmosphere contained no sulfur, cementite decomposition at 925 °C was so fast that it was impossible to convert iron to iron carbide completely. Sulfur stabilized cementite, and the increase in $H_2S$ content in the gas atmosphere increased the cementite content in a sample. When the gas atmosphere contained 0.054 vol pct $H_2S$ (this corresponds to an activity of sulphur in iron of 0.28, the activity of sulfur is assumed to be unity at the Fe/FeS equilibrium with $H_2S$-$H_2$ gas), the degree of iron conversion to cementite was close to one. However, addition of sulfur to the reducing/carburizing gas also retarded cementite formation, so that a further increase in the $H_2S$ content caused a decline in the cementite content.

## B. *Mossbauer Analysis*

The Mossbauer spectra of samples obtained by iron ore reaction with reducing/carburizing gas containing 35 vol pct $CH_4$, 55 vol pct $H_2$, and 10 vol pct Ar during different

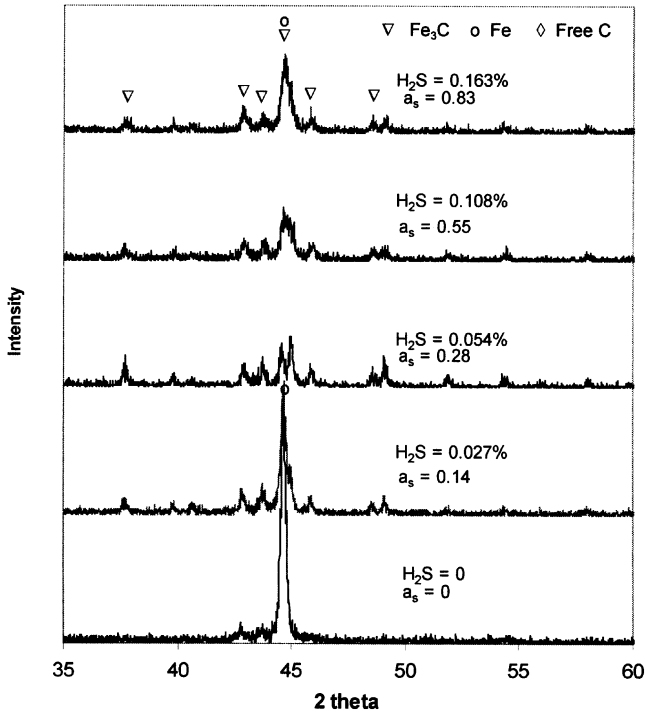


Fig. 5—XRD patterns of samples reduced at 925 °C using $CH_4$-$H_2$-Ar gas (35 vol pct $CH_4$, 55 vol pct $H_2$, and 10 vol pct Ar) with different sulfur additions; all samples were reduced for 1 h.

reaction times at 750 °C are shown in Figure 6. The results are summarized in Table III. After 5 minutes of reaction, the Mossbauer spectrum is a combination of a magnetically-split 6-line subspectrum (sextet with $B_{hf}$ = 3.3 T [Tesla]) due to $\alpha$-Fe, a paramagnetic quadrupole-split doublet in the center of the spectrum corresponding to wustite $Fe_xO$, and two sextets, ($B_{hf}$(A) = 48.8 T and $B_{hf}$(B) = 45.4 T), corresponding to two sites of magnetite. Traces of cementite ($B_{hf}$ = 20.8 T) are also visible. Increasing the reaction time to 15 minutes increased the contents of iron and cementite and decreased the contents of magnetite and wustite. Iron ore was almost completely converted to cementite in about 30 minutes, with a small amount of wustite and metallic iron. Cementite decomposition started after about 1 hour of reaction time, but the decomposition rate was very slow. After 2 hours reaction, the content of cementite was still 83 wt pct.

The XRD (Table II) and Mossbauer analysis (Table III) give close results on cementite fraction over the broad range of cementite contents. However, Mossbauer analysis gives more accurate phase composition in comparison with XRD, especially when the phase content is low.

### C. *XPS Analysis*

The following samples were subjected to the XPS analysis: (1) samples reduced at 835 °C using gas containing 35 vol pct $CH_4$, 55 vol pct $H_2$, and 10 vol pct Ar for 1.5 hours, (2) samples reduced at 925 °C using gas containing 35 vol pct $CH_4$, 55 vol pct $H_2$, 0.054 vol pct $H_2S$, and 10 vol pct Ar for 1 hour, and (3) a Nucor sample. The surfaces of the samples were studied for C 1s core level spectra.

The C 1s binding energies identify carbon in different states, such as segregated (chemisorbed) carbon, graphitic carbon, and carbon in iron carbide.[10–13] Experimental results are presented in Figure 7. The overall C 1s spectra of all three samples were decomposed to two peaks with binding energies shown in Table IV.

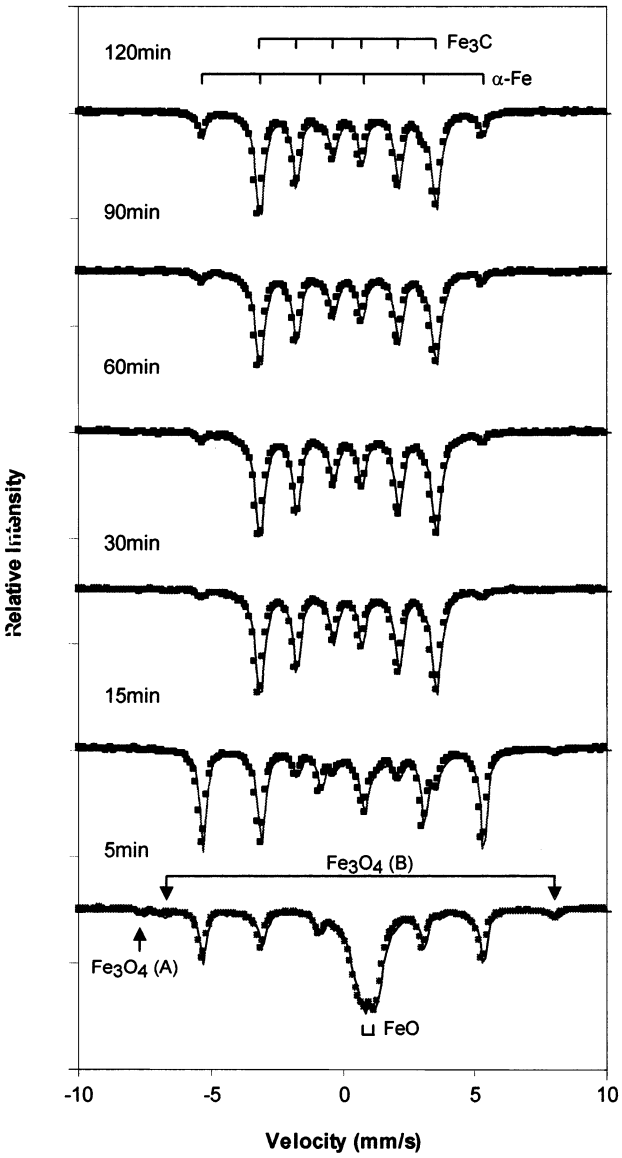


Fig. 6—Mossbauer spectra of samples reduced at 750 °C with $CH_4$-$H_2$-Ar gas (35 vol pct $CH_4$, 55 vol pct $H_2$, and 10 vol pct Ar) as a function of reaction time.

**Table III. Mossbauer Results on Phase Composition of Iron Ore Reduced and Carburized at 750 °C (Weight Percent)**

| | Magnetite | | | | |
|---|---|---|---|---|---|
| Reaction Time (Min) | A site | B site | $Fe_xO$ | Fe | $Fe_3C$ |
| 5 | 2.3 | 4.8 | 46.2 | 43.7 | 3.0 |
| 15 | 0.4 | 1.0 | 25.0 | 52.3 | 21.3 |
| 30 | — | — | 4.2 | 3.9 | 91.9 |
| 60 | — | — | 3.6 | 4.9 | 91.5 |
| 90 | — | — | 3.3 | 6.7 | 90.0 |
| 120 | — | — | 3.2 | 14.3 | 82.5 |

The sample (1) showed no charging effect due to the high free carbon content on the surface, while the peak positions for binding energies of samples (2) and (3) were corrected by considering the charging effect. It was found that surface carbon in a Nucor sample and in a sample reduced with sulfur-containing gas exists in the form of carbide (77 to 83 wt pct) and graphite (17 to 23 wt pct). However, surface carbon in the sample reduced without sulfur was mostly segregated and graphitic carbon. These XPS data on the effect of sulfur on the state of carbon are in accord with XRD and elemental analyses (Figures 3 through 5). Addition of sulfur to the reducing/carburizing gas stabilizes iron carbide and suppresses carbon deposition on the surface.[9,14]

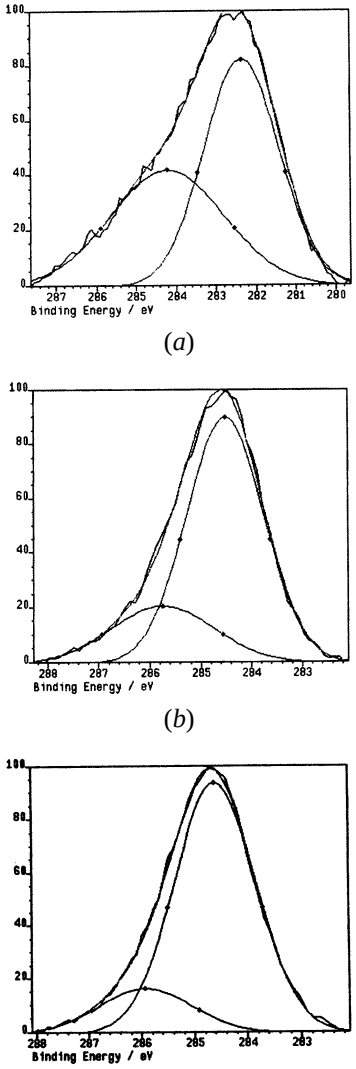


Fig. 7—XPS spectra of (*a*) a sample reduced by sulfur-free $CH_4$-$H_2$-Ar gas, (*b*) a sample reduced in sulfur containing gas atmosphere (35 vol pct $CH_4$, 55 vol pct $H_2$, 10 vol pct Ar, and 0.054 vol pct $H_2S$), and (*c*) a Nucor sample. (Binding energies are given without correction for surface charging.)

## D. *Raman Spectroscopy*

No information on the Raman study of iron carbide was found in literature. Xiang-Xin Bi *et al.*[15] expected to find Raman bands between 200 and 600 $cm^{-1}$, but failed to do so.

The Raman active lattice vibrational modes of an ideal, iron-carbide, single crystal can be calculated by the correlation method.[16] The space group of cementite is *Pnma* and the point group is $D_{2h}^{16}$.[17] The lattice vibrational modes of iron-carbide single crystal, $\Gamma^{Fe_3C}$ are

$$\Gamma^{Fe_3C} = 6A_u + 4B_{1u} + 4B_{2u} + 4B_{3u} \qquad [2]$$

All four modes are Raman inactive.

Samples subjected to Raman analysis were the same as examined by XPS. Raman spectra of a Nucor sample and sample reduced to different extent at 835 °C, using gas containing 35 vol pct $CH_4$, 55 vol pct $H_2$, and 10 vol pct Ar, are shown in Figures 8 and 9, correspondingly. The Raman spectrum of a sample reduced at 925 °C, using gas containing 35 vol pct $CH_4$, 55 vol pct $H_2$, 0.054 vol pct $H_2S$, and 10 vol pct Ar, is presented in Figure 10.

Raman spectra of a partly reduced iron ore contain iron

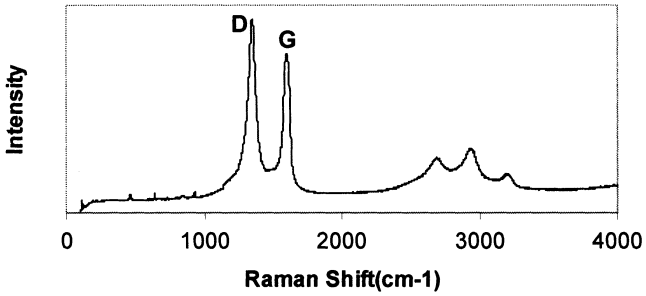


Fig. 8—Raman spectra of a Nucor sample.

**Table IV. C 1 s Binding Energies of Analyzed Samples**

| Sample | Binding Energy (eV), Experimental | Binding Energy (eV), Corrected | FWHM (eV) | Δ (eV) | Wt Pct | Peak |
|---|---|---|---|---|---|---|
| (1) Reduced with $CH_4$-$H_2$-Ar | 282.4 | 282.4 | 2.2 | 1.9 | 56.6 | segregated[12,13] |
| | 284.3 | 284.3 | 3.3 | | 43.4 | graphitic[13] |
| (2) Reduced with $CH_4$-$H_2$-Ar-$H_2S$ | 284.5 | 283.2* | 1.8 | 1.3 | 76.7 | $Fe_3C$[10–13] |
| | 285.8 | 284.5* | 2.3 | | 23.3 | graphitic[10–13] |
| (3) Nucor sample | 284.6 | 283.2* | 1.8 | 1.3 | 83.4 | $Fe_3C$[10–13] |
| | 285.9 | 284.5* | 2.0 | | 16.8 | graphitic[10–13] |

*FWHM: full-width half-maximum.*

*Values corrected by 1.3 eV for sample (2) and 1.4 eV for sample (3), for surface charging. The graphitic carbon binding energy of 284.5 eV was used for these corrections. The value of Δ is the difference of the binding energy between the graphitic carbon and the other identified peak.

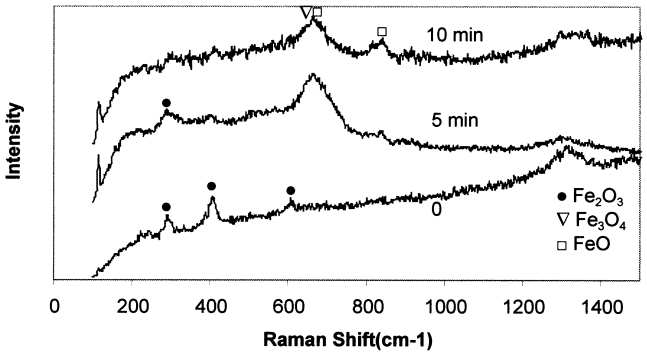


(*a*)

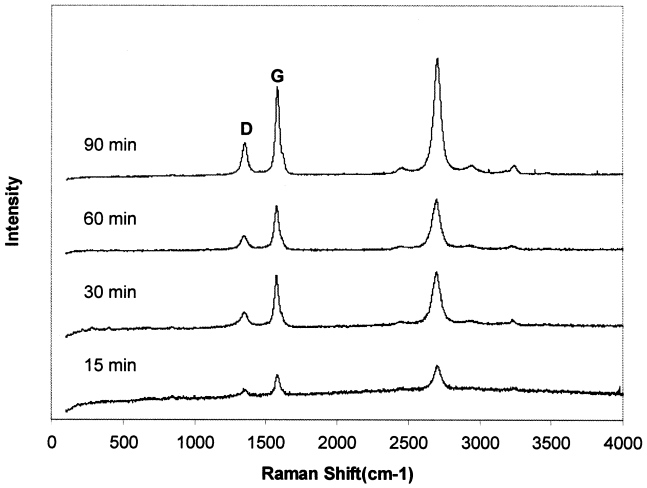


(*b*)

Fig. 9—Raman spectra of samples reduced at 835 °C by $CH_4$-$H_2$-Ar gas (35 vol pct $CH_4$, 55 vol pct $H_2$, and 10 vol pct Ar) at different reduction times: (*a*) in the beginning of the reduction showing iron oxides peaks and (*b*) intermediate and final stages of the reduction showing the peaks from carbon.

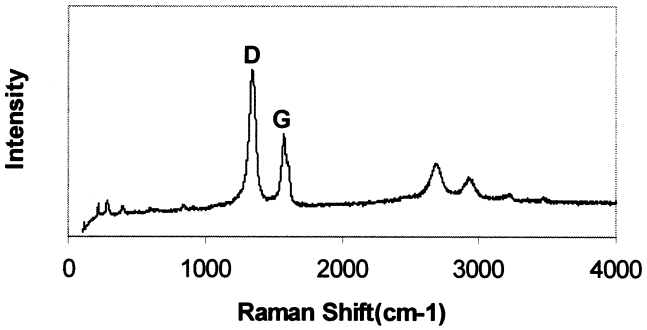


Fig. 10—Raman spectra of a sample reduced at 925 °C by $CH_4$-$H_2$-Ar gas (35 vol pct $CH_4$, 55 vol pct $H_2$, and 10 vol pct Ar) containing 0.054 vol pct $H_2S$.

oxide bands. Characteristic peaks of magnetite and wustite in Raman spectra have very close positions, around 660 $cm^{-1}$.[17,18] However, the peak around 660 $cm^{-1}$ for a sample subjected to 5-minute reduction (Figure 9(a)) can be attributed to wustite, considering XRD results (Figure 3). After 10 minutes of reduction, all hematite was reduced to wustite, and there is no peak from iron oxides after 15 minutes reduction, which means that the reduction of iron oxide was completed in about 15 minutes. In all reduced/carburized samples, two strong peaks were observed at ~1350 and ~1600 $cm^{-1}$. This doublet is attributed to the so-called *D* band and the *G* band of graphite.[15,20–24] Also, two overtones and one combination of *D* and *G* bands were found at ~2700, ~3200, and ~2950 $cm^{-1}$. The *D* band occurs at around 1350 $cm^{-1}$ in amorphous $sp^{2-}$ bonded carbon species, such as pyrolytic graphite, glassy carbon, and carbon powder. In crystalline graphite, only the *G* band is observed at around 1600 $cm^{-1}$. Therefore, the intensity of the *D* band grows with decreasing fraction of graphite. The Raman data show that carbon deposition on a sample surface started before the completion of the reduction process. However, when the reduction was completed, the amount of deposited carbon on a sample surface increased rapidly with the reaction time. This is agreement with results from carbon analysis (Figure 4).

In the process of iron oxide reduction and iron cementation, carbon on the surface of metallic iron, formed as a result of methane cracking, diffuses to a sample interior forming iron carbide. Cementite formed on the sample surface acts as a barrier to the carbon diffusion because the diffusion coefficient of carbon in iron carbide is much smaller than in pure iron.[25] This causes carbon accumulation on the surface and, eventually, cementite decomposition.[9]

The proportions of carbon in the amorphous and graphitic forms can be estimated from the intensity ratio of *D* to *G* bands. The *D*/*G* intensity ratio is above one for a Nucor sample (Figure 8) and a sample reduced by sulfur-containing gas (Figure 10). This means that carbon in these samples predominantly exists in the amorphous phase. Carbon, in a sample reduced by sulfur-free gas, is predominantly in the form of graphite. This supports the Gronebaun and Pluschkell[3] and Zhao *et al.*[26] findings that the surface of synthesized iron carbide is covered with a thin amorphous carbon film. The carbon morphology detected by Raman spectroscopy is in accord with XPS results. However, the origin of the intense overtone of the *D* band at 2700 $cm^{-1}$ is not clear.

## IV. CONCLUSIONS

Phases formed in the process of iron carbide formation by reaction of iron ore with $CH_4$-$H_2$-Ar gas mixtures with and without sulfur at 750 °C, 835 °C, and 925 °C were examined by XRD, Mossbauer, XPS, and Raman spectroscopy. The following phases were identified in samples at different reduction/cementation stages: iron oxides, metallic iron, cementite, and free carbon. Results obtained by XRD and Mossbauer analyses are in a good agreement with one another. Although Mossbauer analysis is more accurate than XRD, particular at a low phase content, XRD is quite acceptable for routine phase analysis.

Surface carbon analyzed by XPS was found to exist in the form of chemisorbed, graphitic carbon, and iron carbide. In a sample reduced by sulfur-containing gas, the predominant form of surface carbon was carbide. In the reduction/cementation of iron ore by sulpfur-free gas, surface carbon was predominantly in the form of chemisorbed and graphitic carbon. This is in agreement with results obtained by Raman spectroscopy. The *D*/*G* intensity ratio of Raman peaks was above one for a sample produced in sulfur-containing gas

atmosphere and below one for a sample obtained in sulfur-free gas. Raman spectroscopy showed that carbon deposition on the sample surface started before the completion of iron oxides reduction.

The XRD, XPS, and Raman spectroscopy results showed that addition of sulfur to the reducing/carburizing gas in the iron carbide process retards cementite formation, stabilizes cementite, and suppresses carbon deposition on the surface.

## ACKNOWLEDGMENTS

Dr. Kiyonori Suzuki's (School of Physics, UNSW, Sydney) assistance in Mossbauer analysis is highly appreciated.

## REFERENCES

1. L. Kolbeinsen and T. Basen: *Metallurgical Processes for Early Twenty-First Century*, H.Y. Sohn, ed. TMS, Warrendale, PA, 1994, pp. 825-42.
2. G.H. Geiger and F.A. Stephens: *1993 Ironmaking Conf. Proc.*, Lakewood, CO, 1993, ISS of AIME, NY, 1993, pp. 333-39.
3. R.H. Gronebaum and W. Pluschkell: *Pre Reduced Products, Int. Conf.*, Milan, Italy, Sept. 23–24, 1996, AIM, Milano, 1996, pp. 204-14.
4. J. Ruer: *Pre Reduced Products, Int. Conf.*, Milan, Italy, Sept. 23–24, 1996, AIM, Milano, 1996, pp. 258-67.
5. R. Garraway: *Iron and Steelmaker*, 1996, vol. 23, pp. 27-30.
6. K.M. Anderson and J. Scheel: *Iron and Steelmaker*, 1997, vol. 24, pp. 25-30.
7. J.O. Edstrom and J. Scheele: *Scand. J. Metall.*, 1997, vol. 26, pp. 196-205.
8. F.M. Stephens, Jr.: *Steel Times Int.*, 1989, July, pp. 18-20.
9. H.J. Grabke and E.M. Muller-Lorentz: *Steel Res.*, 1995, vol. 66, pp. 254-58.
10. V.V. Nemoshkalenko, V.V. Didyk, V.P. Krivitskii, and A.I. Senkevich: *Russ. J. Inorg. Chem.*, 1983, vol. 28, pp. 1239-41.
11. I.N. Shabanova and V.A. Trapeznikov: *J. Elec. Spectr. Related Phenomena*, 1975, vol. 6, pp. 297-307.
12. G. Panzner and W. Diekmann: *Surf. Sci.*, 1985, vol. 160, pp. 253-70.
13. H.J. Grabke: *Iron Steel Inst. Jpn. Int.*, 1989, vol. 29, pp. 529-38.
14. H.J. Grabke, W. Paulitschke, G. Tauber, and H. Viefhaus: *Surf. Sci.*, 1977, vol. 63, pp. 377-89.
15. X.X. Bi, B. Ganguly, G.P. Huffman, F.E. Huggins, M. Endo, and P.C. Eklund: *J. Mater. Res.*, 1993, vol. 8, pp. 1666-74.
16. W.G. Fateley, R.D. Francis, N.T. McDevitt, and F.F. Bentley: *Infrared and Raman Selection Rules for Molecular and Lattice Vibrations: The Correlation Method*, Wiley & Sons, New York, NY, 1972.
17. P. Villars and L.D. Calvert: *Pearson's Handbook of Crystallographic Data for Intermetallic Phases*, ASM International, Materials Park, OH, 1991, vol. 1, p. 1895.
18. D.L.A. de Faria, S.V. Silva, and M.T. de Oliveira: *J. Raman Spectr.*, 1997, vol. 28, pp. 873-78.
19. R.K. Singh Raman, B. Gleeson, and D.J. Young: *Mater. Sci. Technol.*, 1998, vol. 14, pp. 373-76.
20. G. Katagiri, H. Ishida, and A. Ishitani: *Carbon*, 1988, vol. 26, pp. 565-71.
21. T.J. Dines, D. Tither, A. Dehbi, and A. Matthews: *Carbon*, 1991, vol. 29, pp. 225-31.
22. A. Fayer, O. Glozman, and A. Hoffman: *Appl. Phys. Lett.*, 1995, vol. 67, pp. 2299-2301.
23. G.A. Baratta, M.M. Arena, G. Strazzulla, L. Colangli, V. Mennella, and E. Bussoletti: *Nucl. Instrum. Methods in Phys. Res. B*, 1996, vol. 116, pp. 195-99.
24. F. Tuinstra and J.L. Koenig: *J. Chem. Phys.*, 1970, vol. 53, pp. 1126-30.
25. B. Ozturk, V.L. Fearing, J.A. Ruth, and G. Simkovich: *Solid State Ionics*, 1984, vol. 12, pp. 145-51.
26. X.Q. Zhao, Y. Liang, Z.Q. Hu, and B.X. Liu: *J. Appl. Phys.*, 1996, vol. 80, pp. 5857-60.